

## Developmental gene expression differences between humans and mammalian models

Margarida Cardoso-Moreira<sup>1\*</sup>, Britta Velten<sup>2</sup>, Matthew Mort<sup>3</sup>, David N. Cooper<sup>3</sup>, Wolfgang Huber<sup>2</sup>, and Henrik Kaessmann<sup>1\*</sup>

1) Center for Molecular Biology (ZMBH), DKFZ-ZMBH Alliance; Heidelberg University; D-69120 Heidelberg; Germany.

2) Genome Biology Unit; European Molecular Biology Laboratory; D-69117 Heidelberg; Germany.

<sup>10</sup> 3) Institute of Medical Genetics; Cardiff University; Cardiff CF14 4XN; UK.

11

<sup>12</sup> \* Correspondence: M.C.M. (m.moreira@zmbh.uni-heidelberg.de) or H.K. (h.kaessmann@zmbh.uni-  
<sup>13</sup> heidelberg.de).

14 **Abstract**

15 Identifying the molecular programs underlying human organ development and how they differ from  
16 those in model species will advance our understanding of human health and disease.  
17 Developmental gene expression profiles provide a window into the genes underlying organ  
18 development as well as a direct means to compare them across species. We use a transcriptomic  
19 resource for mammalian organ development to characterize the temporal profiles of human genes  
20 associated with distinct disease classes and to determine, for each human gene, the similarity of its  
21 spatiotemporal expression with its orthologs in rhesus macaque, mouse, rat and rabbit. We find  
22 that half of human genes differ from their mouse orthologs in their temporal trajectories. These  
23 include more than 200 disease genes associated with brain, heart and liver disease, for which mouse  
24 models should undergo extra scrutiny. We provide a new resource that evaluates for every human  
25 gene its suitability to be modeled in different mammalian species.

26

27 **Keywords:** human disease, animal models, organogenesis, gene expression.

28

29 **Introduction**

30 The genetic programs underlying human organ development are only partially understood, yet they  
31 hold the key to understanding organ morphology, physiology and disease [1–6]. Gene expression is  
32 a molecular readout of developmental processes and therefore provides a window into the genes  
33 and regulatory networks underlying organ development [7,8]. By densely profiling gene expression  
34 throughout organ development, we get one step closer to identifying the genes and molecular  
35 processes that underlie organ differentiation, maturation and physiology [9–13]. We also advance  
36 our understanding of what happens when these processes are disturbed and lead to disease.  
37 Spatiotemporal gene expression profiles provide a wealth of information on human disease genes,  
38 which can be leveraged to gain new insights into the etiology and symptomatology of diseases  
39 [8,14–16].

40

41 Much of the progress made in unraveling the genetic programs responsible for human organ  
42 development has come from research in model organisms. Mice and other mammals (e.g., rats and  
43 rhesus macaques) are routinely used as models of both normal human development and human  
44 disease because it is generally assumed that the genes and regulatory networks underlying  
45 development are largely conserved across these species. While this is generally true, there are also  
46 critical differences between species during development, which underlie the large diversity of

47 mammalian organ phenotypes [1–6,8]. Identifying the commonalities and differences between the  
48 genetic programs underlying organ development in different mammalian species is therefore  
49 paramount for assessing the translatability of knowledge obtained from mammalian models to  
50 understand human health and disease. Critically, gene expression profiles can be directly compared  
51 between species, especially when they are derived from matching cells/organs and developmental  
52 stages. Gene expression therefore offers a direct means to evaluate similarities and differences  
53 between species in organ developmental programs. While the relationship between gene  
54 expression and phenotypes is not linear, identifying when and where gene expression differs  
55 between humans and other species will help identify the conditions (i.e., developmental stages,  
56 organs, genes) under which model species may not be well suited to model human development  
57 and disease.

58

59 Here, we take advantage of a developmental gene expression resource [13], which densely covers  
60 the development of seven major organs in humans and other mammals, to characterize the  
61 spatiotemporal profiles of human disease genes and gain new insights into the symptomatology of  
62 diseases. We also determine for each human gene (including disease-associated genes) the  
63 similarity of its spatiotemporal expression with that of its orthologs in mouse, rat, rabbit and rhesus  
64 macaque. Our analyses and datasets therefore provide a new resource for assessing the suitability  
65 of different mammalian species to model the action of individual genes and/or processes in both  
66 healthy and pathological human organ development.

67

## 68 Results

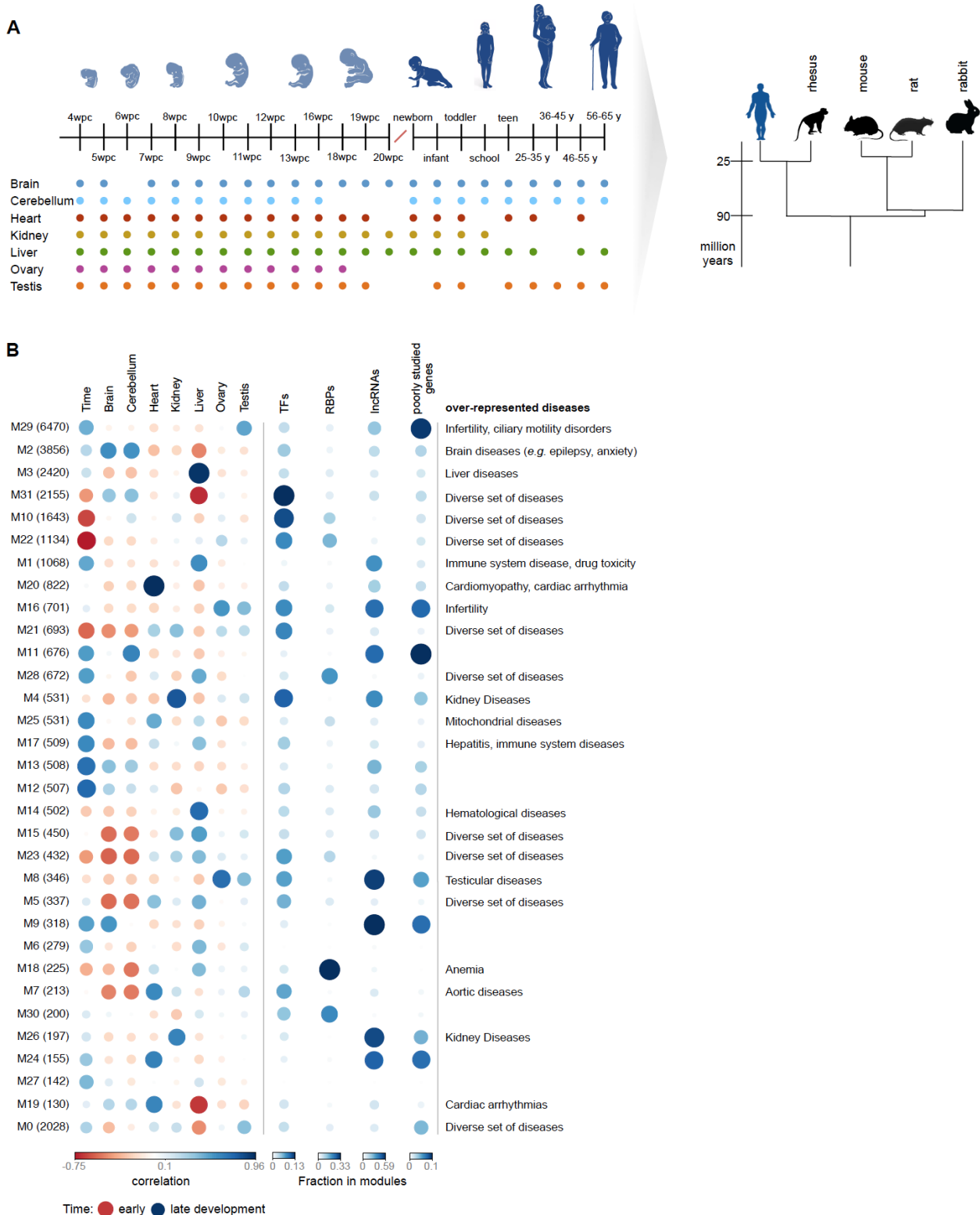
### 69 An expression atlas of human organ development

70 The resource [13] provides human gene expression time series for seven major organs: brain  
71 (forebrain/cerebrum), cerebellum (hindbrain/cerebellum), heart, kidney, liver, ovary and testis  
72 (Figure 1A). The time series start at 4 weeks post-conception (wpc), which corresponds to early  
73 organogenesis for all organs except the heart (mid-organogenesis), and then cover prenatal  
74 development weekly until 20 wpc. The sampling restarts at birth and spans all major developmental  
75 milestones, including ageing (Figure 1A; total of 297 RNA-sequencing (RNA-seq) libraries). Matching  
76 datasets are available for mouse (316 libraries), rat (350 libraries) and rabbit (315 libraries) until  
77 adulthood and for rhesus macaque starting at a late fetal stage (i.e., embryonic (e) day 93,  
78 corresponding to 19 wpc human [13]; 154 libraries; Methods).

79

80 We used weighted gene co-expression network analysis to identify the main clusters (modules) of  
81 highly correlated genes during human organ development (Methods). We then characterized each  
82 module according to its developmental profile (Figure 1B; Figure S1A), functional and disease  
83 enrichments (Figure 1b; Table S1), and proportion of transcription factors (TFs) [17], RNA-binding  
84 proteins (RBPs) [18] and developmentally dynamic long noncoding RNAs (lncRNAs) [19] (Figure 1B).  
85 As expected, there is a clear match between the disease enrichments of each module and its organ  
86 developmental profile (Figure 1B). For example, module M3 comprises 2,420 genes mainly  
87 expressed in the liver and it is associated with a number of liver-related diseases (e.g., fatty liver).  
88 Module M20 (822 genes) comprises genes mainly expressed in the heart and is associated with a  
89 number of cardiomyopathies. Consistent with previous work [13], we observe that modules  
90 associated with higher expression early in development have a significantly higher fraction of TFs  
91 than modules associated with higher expression late in development (Pearson's  $\rho$ : -0.71,  $P$ -value =  
92  $5 \times 10^{-6}$ ; Figure S1B), a result that is consistent with TFs directing most of organogenesis. The  
93 modules identified also provide a wealth of information on poorly characterized genes, that through  
94 "guilt-by-association" can be assigned putative functions (Table S2). We identified a strong positive  
95 correlation between the fraction of protein-coding genes in a module that are among the least  
96 studied in the human genome [20] and the module's fraction of dynamic lncRNAs ( $\rho$ : +0.77,  $P$ -value  
97 =  $2 \times 10^{-7}$ ). Modules rich in dynamic lncRNAs and poorly studied protein-coding genes are frequently  
98 associated with high expression in the gonads (Figure 1B) but are also found in association with high  
99 expression in each of the other organs (e.g., module M9 for brain and module M11 for cerebellum).  
100  
101 The breadth of developmental expression (i.e., the organ- and time-specificity of a gene) informs on  
102 gene function, because it is expected to correlate with the spatiotemporal manifestation of  
103 phenotypes. TFs, RBPs and members of the seven major signaling pathways all play key roles during  
104 development but have distinct spatiotemporal profiles (Figure S2; time- and organ-specificity are  
105 strongly correlated [13]). Consistent with previous observations [18], RBPs are generally  
106 ubiquitously expressed, with only 6% (100) showing time- and/or organ-specificity (Figure S3).  
107 Among these are the developmental regulators LIN28A and LIN28B, which are expressed at the  
108 earliest stages across somatic organs; the heart-specific splicing factor RMB20, which has been  
109 associated with cardiomyopathy; gonad-specific RBPs predicted to bind to piRNAs; and several  
110 members of the ELAV family of neuronal regulators. Signaling genes also tend to be ubiquitously  
111 expressed (Figure S2), but they include a higher fraction (19-20%) of time- and/or organ-specific  
112 genes than RBPs. As expected, the greatest variation in the breadth of spatiotemporal expression is

113 found among classes of TFs (Figure S2). Myb TFs are mostly ubiquitously expressed (Figure S4),  
114 whereas homeobox, POU-homeobox (Figure S5) and forkhead (Figure S6) TFs display high time- and  
115 organ-specificity (Figure S2). Although only 16% of zinc finger TFs show spatiotemporal specificity,  
116 they constitute ~1/4 of all time- and/or organ-specific TFs due to their high abundance. Another  
117 ~1/4 corresponds to homeobox TFs, and the remaining half derive from various classes of TFs.  
118 Notable among homeobox TFs are the Hox genes, which are critical for pattern specification at the  
119 earliest stages of development [21]. In the developmental span examined in our study, Hox genes  
120 play an important role during the development of the urogenital system and the early hindbrain  
121 (but not cerebrum) (Figure S7).



122

**Figure 1. An expression atlas of human organ development.** **(A)** Description of the dataset. The dots mark the sampled stages in each organ (median of 2 replicates). **(B)** Modules in the gene co-expression network (number of genes in each module in parentheses), their correlation with organs and developmental time (full developmental profiles in Figure S1A), their fraction of TFs, RBPs, developmentally dynamic lncRNAs and poorly studied protein-coding genes, and examples of overrepresented diseases (FDR < 1%, hypergeometric test; Table S1). The modules are ordered vertically by decreasing number of genes. Module 0 (bottom) includes genes not assigned to any of the other modules.

129 **Spatiotemporal profiles of disease genes**

130 The breadth of developmental expression can also inform on the etiology and phenotypic  
131 manifestation of human diseases. We integrated a dataset of human essential genes [22] with the  
132 set of genes associated with inherited disease in the manually curated Human Gene Mutation  
133 Database (“disease genes”) [23] to compare the breadth of developmental expression of genes in  
134 distinct classes of phenotypic severity (Figure 2A). We found a clear association between expression  
135 pleiotropy (i.e., fraction of total samples in which genes are expressed) and the severity of  
136 phenotypes (Figure 2B). Essential genes that are not associated with disease are likely enriched for  
137 embryonic lethality and are, congruently, the most pleiotropic. Genes that when mutated range  
138 from lethality to causing disease (often developmental disorders affecting multiple organs) are less  
139 pleiotropic than embryonic lethals but are more pleiotropic than genes only associated with disease  
140 (both  $P$ -value =  $2 \times 10^{-16}$ , Wilcoxon rank sum test, two-sided; Figure 2B). Finally, non-lethal disease  
141 genes are more pleiotropic than genes not associated with deleterious phenotypes ( $P$ -value =  $2 \times$   
142  $10^{-5}$ ; Figure 2B). A similar association is obtained when looking independently at organ- and time-  
143 specificity (Figure S8A).

144

145 Human diseases differ in terms of severity, age of onset and organs affected, all of which should be  
146 reflected in the spatiotemporal expression profiles of underlying disease genes. We therefore  
147 looked at the time- and organ-specificity of genes associated with different classes of disease [23]  
148 (Figure 2C). As expected, the specificity of the spatiotemporal profiles of disease genes differs  
149 considerably among disease classes. Genes implicated in developmental disorders, cancer and  
150 diseases of the nervous system tend to be ubiquitously expressed (spatially and temporally),  
151 whereas genes causing heart and reproductive diseases tend to have more restricted expression  
152 (Figure 2C). Further insights were obtained by analysing the temporal trajectories of disease genes  
153 within the organs they affect. We used a soft clustering approach to identify the most common  
154 expression profiles in each organ and assigned each gene a probability of belonging to each of the  
155 clusters (Methods; Table S2). Disease genes are enriched within specific clusters, which are disease  
156 and organ-specific. For example, genes associated with heart disease are significantly enriched  
157 among genes characterized by a progressive increase in expression throughout heart development,  
158 whereas genes associated with metabolic diseases are enriched among genes that exhibit a strong  
159 up-regulation in the liver in the first months after birth (Figure S8B-C).

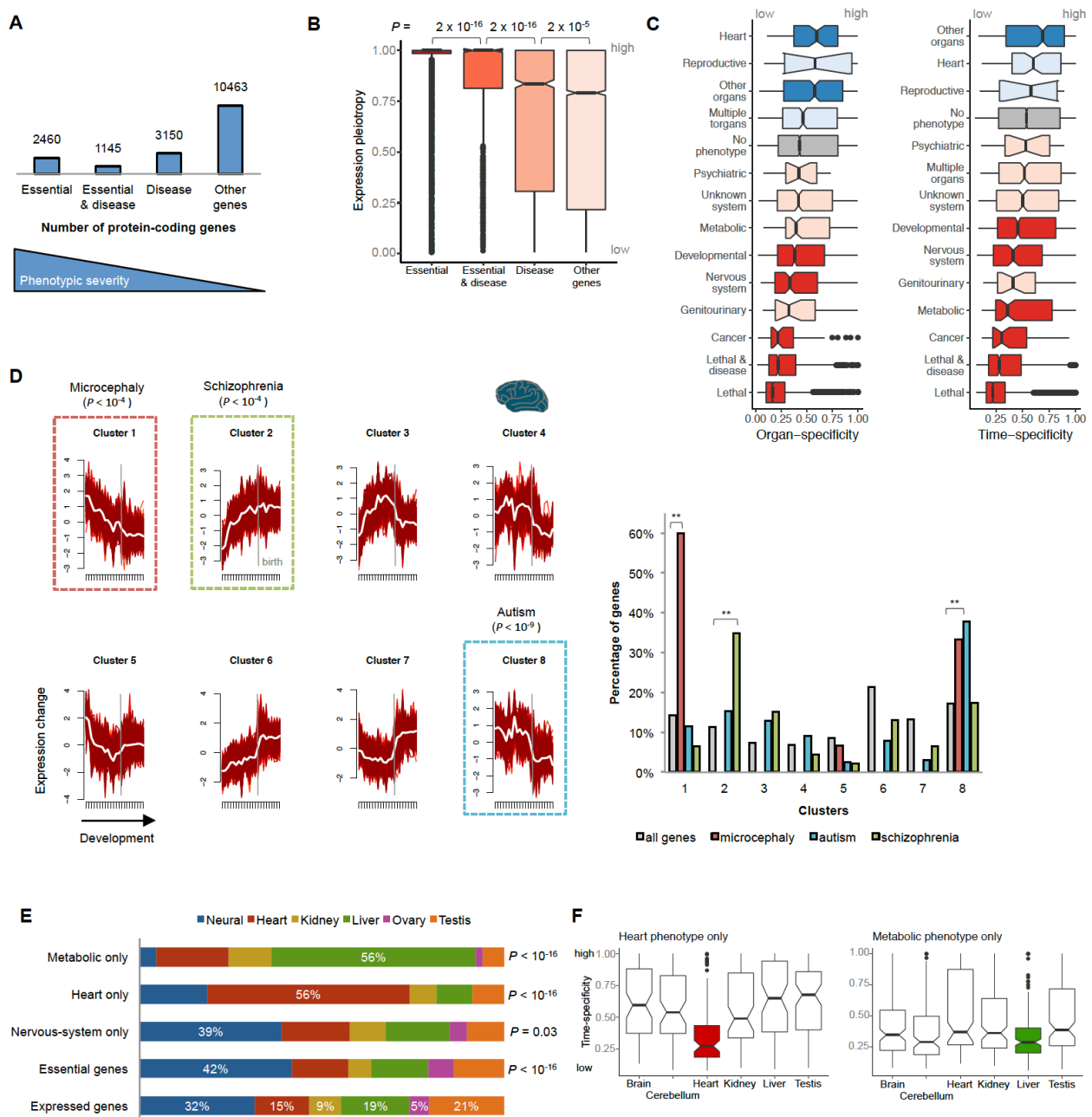
160

161 Within the brain, we focused on the temporal trajectories of genes associated with three  
162 neurodevelopmental disorders: primary microcephaly, autism and schizophrenia (Methods).  
163 Consistent with these disorders having different etiologies and ages of onset, the associated genes  
164 are significantly enriched among distinct temporal profiles in the brain (Figure 2D). Genes causing  
165 primary microcephaly show their highest expression at the earliest developmental stages followed  
166 by a progressive decrease in expression, whereas genes implicated in schizophrenia show the  
167 opposite profile: a progressive increase in expression throughout development (Figure 2D). Genes  
168 associated with autism are expressed throughout prenatal development and subsequently display  
169 a sharp decrease in expression near birth (Figure 2D). The two temporal profiles in the brain that  
170 are enriched with microcephaly- and autism-associated genes are also enriched with essential genes  
171 ( $P$ -value  $< 10^{-16}$ , binomial test).

172

173 Most (86%) disease genes that we analyzed are associated with phenotypes in multiple organs, but  
174 this still leaves hundreds of genes that affect exclusively one organ. Many of these genes present a  
175 puzzle in biomedical research because, as previously noted [24,25], they are not expressed in an  
176 organ-specific manner. Our analysis of developmental transcriptomes further strengthens this  
177 puzzle. Genes known to cause organ-specific phenotypes exhibit dynamic temporal profiles in a  
178 similar number of organs as genes causing phenotypes across multiple organs (i.e., median of 4  
179 organs for both gene sets; Figure S9A). This raises the question as to why mutations that mostly  
180 disrupt the coding-sequences of genes temporally dynamic in multiple organs lead to diseases that  
181 are organ-specific. A number of different factors may explain this phenomenon, including  
182 alternative splicing (e.g., mutations may affect only organ-specific isoforms) [26], functional  
183 redundancy [25], and/or dependency on the characteristics of specific cell types (e.g., protein-  
184 misfolding diseases in long-lived neurons). It has also been suggested that pathologies tend to be  
185 associated with the organ where the genes display elevated expression [24]. This prompted us to  
186 ask where genes associated with organ-specific diseases exhibit their maximum expression during  
187 development. We focused on heart, neurodevelopmental, psychiatric, and metabolic diseases (the  
188 latter tested in association with the liver). We found a strong association between the organ of  
189 maximum expression during development and the organ where the pathology manifests (Figure  
190 2E). Thus, we found that 56% of the genes exclusively associated with heart disease show maximal  
191 expression in the heart (vs. 15% for all genes,  $P$ -value =  $2 \times 10^{-16}$ , binomial test; Figure 2E), that 56%  
192 of the genes with an exclusively metabolic phenotype show maximal expression in the liver (vs. 19%  
193 for all genes,  $P$ -value =  $2 \times 10^{-16}$ ; Figure 2E), and that genes exclusively associated with

194 neurodevelopmental diseases are enriched for maximal expression in the brain (39% vs. 32% for all  
195 genes,  $P$ -value = 0.03; Figure 2D). The duration of gene expression may also help to explain organ-  
196 specific pathologies, at least for heart disease. Genes expressed in multiple organs that have heart-  
197 specific phenotypes are ubiquitously expressed during heart development but show a significantly  
198 higher time-specificity (i.e., shorter expression window) in the other organs (all  $P$ -value <  $10^{-4}$ ,  
199 Wilcoxon rank sum test, two-sided; Figure 2F). We note, however, that time-specificity does not  
200 help to explain metabolic- or neurodevelopmental-specific phenotypes, as we see no difference in  
201 the time-specificity of genes in the affected organs versus the others (Figure 2F; Figure S9B). Overall,  
202 the association of pathology with level of gene expression, and to a lesser extent with duration of  
203 gene expression, suggest that the development of organ-specific pathologies can at least in some  
204 cases be explained by differences in the abundance (spatial and/or temporal) of the cell type(s) that  
205 express the mutated gene in the different organs.



206

207 **Figure 2. Spatiotemporal profiles of disease genes.** (A) Number of expressed (RPKM > 1) protein-coding genes in  
208 different classes of phenotypic severity. (B) Expression pleiotropy of genes in different classes of phenotypic severity  
209 (P-values from Wilcoxon rank sum test, two-sided). (C) Organ- and time-specificity (median across organs) of genes  
210 associated with different classes of diseases. In red are diseases associated with genes with time/organ-specificity lower  
211 than non-disease-associated genes and in blue those with higher (darker colors mean that the difference is significant,  
212  $P \leq 0.05$ , Wilcoxon rank sum test, two-sided). (D) Genes associated with primary microcephaly ( $n = 15$ ), autism ( $n = 164$ )  
213 and schizophrenia ( $n = 46$ ) are significantly enriched (binomial test) in distinct expression clusters in the brain (on the  
214 left are the clusters identified through soft clustering of the brain developmental samples). The genes associated with  
215 each disorder are significantly enriched in only one of the 8 clusters (right). (E) Organs where genes associated with  
216 organ-specific phenotypes show maximum expression. P-values from binomial tests. (F) Time-specificity in the different  
217 organs of genes with heart- and metabolic-specific phenotypes. In (B), (C) and (F), the box plots depict the median  $\pm$   
218 the 25th and 75th percentiles, with the whiskers at 1.5 times the interquartile range.

219 **Presence/absence expression differences are rare between species**

220 The extensive use of mice, rats and other mammals in biomedical research is predicated upon the  
221 assumption of an overall conservation of developmental programs between humans and these  
222 species. This assumption has been largely supported by comparative analyses of developmental  
223 expression profiles [13] and by comparative analyses of the human and mouse trans-acting  
224 regulatory circuitry [27]. However, this broad conservation does not preclude developmental  
225 expression differences in individual genes that can profoundly impact the translatability of  
226 phenotypes between humans and other species.

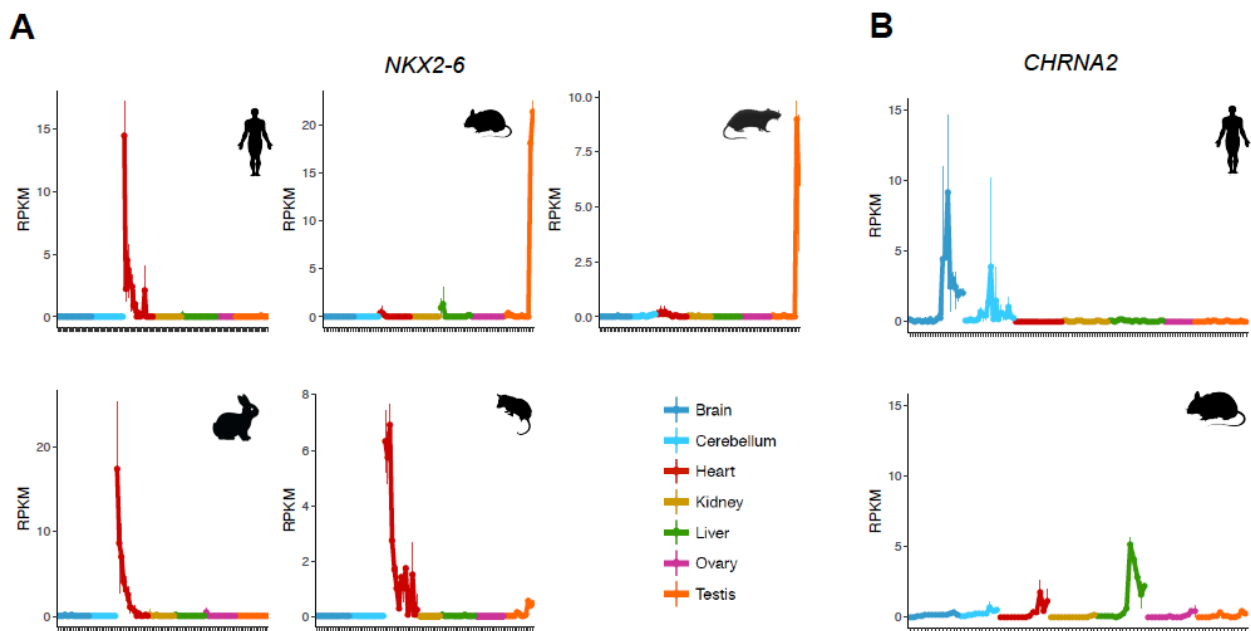
227

228 We first compared human genes and their orthologs in mouse, rat, rabbit and rhesus macaque in  
229 terms of stark differences in spatiotemporal profiles: presence/absence of gene expression in a  
230 given organ and large differences in expression pleiotropy across multiple organs. Differences  
231 between humans and each of the other species in terms of the presence or absence of gene  
232 expression in an organ are rare. In a comparison of human and mouse, only 1-3% of protein-coding  
233 genes (177 – 372 genes depending on the organ) are robustly expressed ( $\text{RPKM} \geq 5$ ) in human but  
234 not in mouse ( $\text{RPKM} \leq 1$ ). These percentages are similar for the comparisons with the other species  
235 (i.e., 1-2% of genes robustly expressed in human are not expressed in rat/rabbit/rhesus macaque).  
236 Although rare, these differences also include disease genes. For example, among genes robustly  
237 expressed in heart in human but not in mouse are 17 genes associated with heart disease. These  
238 include *NKX2-6*, which causes conotruncal heart malformations in human [28] that, congruently, are  
239 not recapitulated by a mouse knockout [29]. The developmental profile of *NKX2-6* in the human  
240 heart is ancestral; the heart expression was lost specifically in rodents, and this is therefore an  
241 example of a disease gene that would probably be better studied in the rabbit (Figure 3A). Genes  
242 associated with neurological diseases are depleted among the set of genes expressed in the human  
243 but not in the mouse brain (12 differ vs. 28 expected,  $P\text{-value} = 4 \times 10^{-4}$ , binomial test). Among the  
244 exceptions is *CHRNA2*, a gene expressed in the human brain starting at birth that has been  
245 implicated in epilepsy [30,31]. Once again, and congruently, this clinical phenotype is not  
246 recapitulated in the mouse knockout [29] (Figure 2B).

247

248 The global breadth of spatiotemporal expression is also very similar between human genes and their  
249 orthologs in mouse, rat, rabbit and rhesus macaque. They are highly correlated in terms of their  
250 organ-specificity (Pearson's  $r = 0.85\text{--}0.86$ , all  $P\text{-value} < 10^{-16}$ ), time-specificity ( $r = 0.68\text{--}0.84$  for  
251 individual organs and  $0.83\text{--}0.84$  for median time-specificity, all  $P\text{-value} < 10^{-16}$ ) and, therefore, for

252 global expression pleiotropy ( $r = 0.84\text{-}0.90$ , all  $P$ -value  $< 10^{-16}$ ). There are only 141 genes expressed  
253 in at least half the human samples but in fewer than 10% of the mouse samples, and 172 genes with  
254 the opposite pattern (Figure S9C). These genes are depleted for essential genes ( $P$ -value =  $8 \times 10^{-6}$ ,  
255 binomial test) and disease genes ( $P$ -value = 0.02, binomial test). Overall, differences in the breadth  
256 and presence/absence of gene expression between humans and other species are confined to a  
257 small set of genes. However, when present, they can translate into relevant phenotypic differences.



258  
259 **Figure 3. Suitability of the mouse as a model.** (A) Developmental profile of *NKX2-6* in human, mouse, rat, rabbit and  
260 opossum. *NKX2-6* is robustly expressed in the human heart but not in mouse, and the conotruncal heart malformations  
261 observed in human are not recapitulated by a mouse knockout. The human heart profile of *NKX2-6* is ancestral as it is  
262 similar to the profiles in rabbit and opossum. (B) Developmental profile of *CHRNA2* in human and mouse. *CHRNA2* is  
263 robustly expressed in the human brain but not in mouse, and the epileptic phenotypes observed in human are not  
264 recapitulated by a mouse knockout.

265

#### 266 Organ-specific temporal differences are common

267 It is not uncommon for genes with broad spatiotemporal profiles to evolve new organ  
268 developmental trajectories in specific species or lineages [13]. Differences between mammalian  
269 species in organ developmental trajectories were first identified using a phylogenetic approach that  
270 included distantly related species (i.e., the marsupial opossum which diverged from human ~160  
271 million years ago [32]) [13]. Therefore, only a restricted set of human genes was evaluated for  
272 potential trajectory differences (e.g., 3,980 genes in the brain). Here, we compared the human  
273 developmental profiles in each of the organs with their orthologs in mouse, rat, rabbit and rhesus  
274 macaque in a pairwise manner (Methods; Tables S3-S8; because of the shorter rhesus macaque's

275 time series, this analysis was only performed for brain, heart and liver). This allowed us to duplicate  
276 or triplicate (depending on the organ) the number of orthologous genes analyzed for differences in  
277 their developmental trajectories. Figure 4A shows examples of genes with different developmental  
278 trajectories between human and mouse.

279

280 Consistent with the original study [13], we found differences between the organs in the proportion  
281 of genes with trajectories differences between humans and each of the other species (Figure 4B):  
282 differences are highest in testis and liver and lowest in brain. There are also expected differences  
283 between species: a smaller fraction of genes differs between human and rhesus macaque (diverged  
284 ~29 million years ago) than between human and each of the glires (diverged ~90 million years ago).  
285 However, we also identified a higher proportion of genes that differ between human and mouse  
286 than between human and rabbit (despite the same divergence time), a result consistent with the  
287 original observation that rodents have evolved a larger number of trajectory differences [13].

288

289 Genes with different developmental trajectories between human and mouse are common: 51% of  
290 the genes tested differ in at least one organ. Most of these genes (67%) differ in only one organ  
291 (25% of genes differ in two organs, and 8% differ in 3 or more), despite on average showing dynamic  
292 temporal profiles in 5-6 organs. Genes with differences in developmental trajectories are depleted  
293 for TFs ( $P$ -value =  $2 \times 10^{-5}$ , Fisher's exact test, two-sided) and are functionally enriched for protein  
294 metabolism (Benjamini-Hochberg corrected  $P$ -value =  $1 \times 10^{-4}$ , overrepresentation enrichment  
295 analysis). Interestingly, genes with different trajectories in the brain (but not in the other organs)  
296 are enriched among a set of genes identified as carrying signs of positive-selection in their coding-  
297 sequences across mammalian species [33] ( $P$ -value = 0.008, Fisher's exact test).

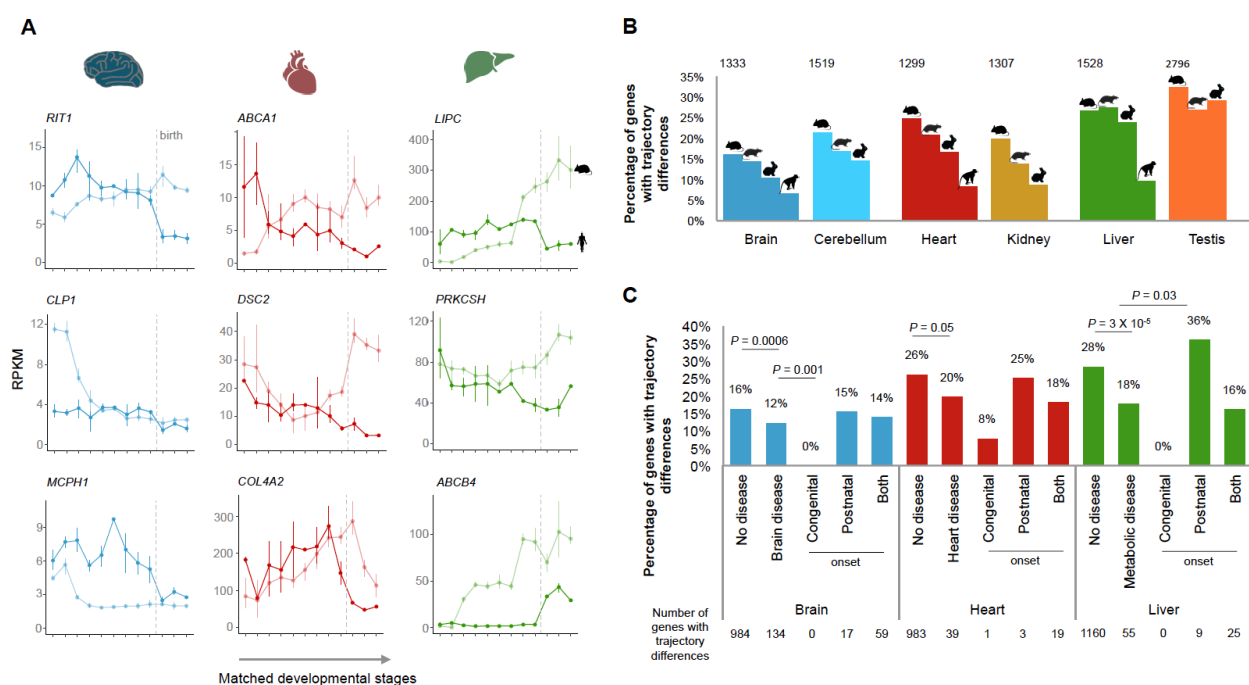
298

299 The genes depicted in Figure 4A are associated with diseases that affect the organ in which human  
300 and mouse display different trajectories. For these genes, the disease etiology may not be fully  
301 recapitulated by mouse models. The mouse knockouts are still expected to affect the development  
302 of the organ associated with the disease, but the cellular and developmental context of the  
303 phenotypes in mouse could differ substantially from those in human. It is therefore noteworthy that  
304 genes associated with human disease are less likely than non-disease genes to differ in their  
305 trajectories between human and mouse (Figure 4C; and between human and the other species; data  
306 not shown). Genes causing diseases that affect the brain, heart and liver are significantly depleted  
307 for trajectory differences between human and mouse in each of the organs (Figure 4C,  $P$ -value =

308 0.0006 for the brain,  $P$ -value = 0.05 for the heart and  $P$ -value =  $3 \times 10^{-5}$  for the liver, Fisher's exact  
309 test). Nevertheless, that leaves more than 200 disease genes whose developmental profiles may  
310 not be fully recapitulated in the mouse (Figure 4C).

311

312 We also posed the question as to whether genes underlying diseases with different ages of onset  
313 are equally likely to differ between human and mouse. Although the number of disease genes  
314 associated with an exclusive congenital or exclusive postnatal onset is low, we found that genes  
315 with congenital onsets almost never differ in terms of their developmental trajectories between  
316 human and mouse (i.e., only 1 out of 82 genes causing disease in the brain, heart or liver; Figure 4C)  
317 whereas genes with postnatal onsets are more likely to show differences (although this difference  
318 is only statistically significant for the liver,  $P$ -value = 0.03, binomial test; Figure 4C). Overall, we  
319 suggest that for genes with differences in developmental trajectories (Tables S3-S8), existing mouse  
320 models of human diseases should undergo extra scrutiny and the possibility of studying alternative  
321 models should be carefully considered.



322

323 **Figure 4. Developmental trajectory differences.** **(A)** Examples of human disease genes with different developmental  
324 trajectories between human and mouse in the affected organ. **(B)** Percentage of genes in each organ that have different  
325 trajectories between human and mouse, rat, rabbit and rhesus. On the top are the number of genes that have a different  
326 trajectory between human and mouse. **(C)** Percentage of genes in brain, heart and liver that differ in trajectories  
327 between human and mouse.  $P$ -values for comparisons between disease and non-disease genes are from Fisher's exact  
328 tests and  $P$ -values for comparisons of disease genes with different ages of onset are from binomial tests.

329

330

331 **Discussion**

332 We integrated datasets of human essential and disease genes with developmental gene expression  
333 profiles in order to shed new light on the causes and phenotypic manifestations of human diseases.  
334 We found that the breadth of spatiotemporal expression correlates positively with the severity of  
335 phenotypes and that it differs considerably among genes associated with different disease classes.  
336 We also found that disease-associated genes are enriched within specific developmental modules  
337 in the organs affected, and that genes associated with different brain developmental disorders show  
338 distinct temporal profiles during brain development. There is therefore a clear association between  
339 spatiotemporal profiles and the phenotypic manifestations of diseases.

340

341 The analysis of developmental transcriptomes further strengthened the apparent paradox of  
342 ubiquitously expressed genes often having organ-specific phenotypes [24,25]. We could not  
343 distinguish genes associated with organ-specific phenotypes from those associated with multi-  
344 organ phenotypes based on the breadth of spatiotemporal profiles. However, for genes associated  
345 with organ-specific phenotypes, there is a strong association between the organ affected and the  
346 organ of maximal expression during development. This association suggests that at least some  
347 organ-specific pathologies could be explained by differences between organs in the spatial and  
348 temporal abundance of the cells expressing the mutated gene.

349

350 Gene expression links genes with their organismal phenotypes and hence offers a direct means to  
351 compare both across species. It can, therefore, inform on the likelihood that insights obtained from  
352 studies in model species are directly transferable to human. We found that stark changes in gene  
353 expression (e.g., presence/absence of expression) are rare between species. However, they do  
354 sometimes occur in disease genes, and in these cases, they may explain why for these genes mouse  
355 models fail to recapitulate the human phenotypes. Strikingly, we also found that differences  
356 between humans and other species in terms of the genes' temporal trajectories during organ  
357 development are common. About half of human genes exhibit a different developmental trajectory  
358 from their mouse orthologs in at least one of the organs. In further support of the use of model  
359 organisms for disease research, we found that disease genes are less likely to differ than the average  
360 gene. Nevertheless, we still identified more than 200 genes known to be causally associated with  
361 brain, heart and/or liver disease, that differ in developmental trajectories between human and  
362 mouse in the affected organ.

363

364 Different reasons, that are not mutually exclusive, can account for the differences in temporal  
365 trajectories observed between species. Differences in developmental trajectories can be created by  
366 gene expression differences between species in homologous cell types, differences between species  
367 in cellular composition, and/or differences between species in the cell types that express  
368 orthologous genes. All of these differences can decrease the likelihood that the phenotype  
369 associated with a human gene will be fully recapitulated in a model species. However, differences  
370 in trajectories created by changes in the identity of the cell types that express an orthologous gene  
371 in different species will lead to the greatest phenotypic divergence. Endeavors that seek to clarify  
372 the causes of trajectory differences therefore represent a key next step, given that they will identify  
373 further genes and processes that are challenging to model in other species. The use of single-cell  
374 technologies will greatly aid these efforts [34].

375

376 Gene expression is only one of several steps connecting genes to their phenotypes. Similarities and  
377 differences in gene expression between species will not always translate into conserved and  
378 divergent phenotypes, respectively. This notwithstanding, detailed comparisons of developmental  
379 gene expression profiles, as performed here, can substantially help to assess the translatability of  
380 the knowledge gathered on individual genes from model species to humans.

381

## 382 Acknowledgments

383 We thank S. Anders, R. Arguello, I. Sarropoulos, M. Sanchez Delgado, M. Sepp, T. Studer, Y. E. Zhang  
384 and members of the Kaessmann group for discussions. D.N.C and M.M. are in receipt of financial  
385 support from Qiagen through a License Agreement with Cardiff University. This research was  
386 supported by grants from the European Research Council (615253, OntoTransEvol) and Swiss  
387 National Science Foundation (146474) to H.K, and Marie Curie FP7-PEOPLE-2012-IIF to M.C.M.  
388 (329902).

389

## 390 Author Contributions

391 M.C.M. and H.K. conceived the study. M.C.M. performed the analyses. M.C.M. wrote the  
392 manuscript, with input from all authors. B.V. and W.H. contributed to the analyses on trajectory  
393 differences. M.M. and D.N.C. contributed to the analyses on human inherited disease.

394

## 395 Declaration of Interests

396 The authors declare no competing interests.

397 **Methods**

398 **Resource**

399 From a mammalian resource on organ development [13], we analyzed data from 1,443 strand-  
400 specific RNA-seq libraries sequenced to a median depth of 33 million reads: 297 from human, 316  
401 from mouse (outbred strain CD-1 - RjOrl:SWISS), 350 from rat (outbred strain Holtzman SD), 315  
402 from rabbit (outbred New Zealand breed) and 165 from rhesus macaque. The organs,  
403 developmental stages and replicates sampled in each species are described in Table S9. The mouse  
404 time series started at e10.5 and there were prenatal samples available for each day until birth (i.e.,  
405 e18.5). There were postnatal samples for 5 stages: P0, P3, P14, P28 and P63. The rat time series  
406 started at e11 and there were prenatal samples available for each day until birth (i.e., e20). There  
407 were postnatal samples for 6 stages: P0, P3, P7, P14, P42 and P112. The rabbit time series started  
408 at e12 and there were 11 prenatal stages available up to and until e27 (gestation lasts ~ 29-32 days).  
409 There were postnatal samples for 4 stages: P0, P14, P84 and P186-P548. Finally, the time series for  
410 rhesus macaque started at a late fetal stage (e93) and there were 5 prenatal stages available up to  
411 and until e130 (gestation last ~ 167 days). There were postnatal samples for 8 stages: P0, P23, 5-6  
412 months of age, 1 year, 3 years, 9 years, 14-15 years, and 20-26 years. For mouse, rat and rabbit  
413 there were typically 4 replicates (2 males and 2 females) per stage, except for ovary and testis (2  
414 replicates). For human and rhesus macaque, the median number of replicates was 2.

415

416 **Gene co-expression networks**

417 We built gene co-expression networks using weighted correlation network analysis (WGCNA 1.61)  
418 [35]. We used as input data the read counts after applying the variance stabilizing (VS)  
419 transformation implemented in DESeq2 (1.12.4) [36]. Each stage was represented by the median  
420 across replicates. In addition to protein-coding genes, we included a set of 5,887 lncRNAs that show  
421 significant differential temporal expression in at least one organ and that show multiple signatures  
422 for being enriched with functional genes [19]. We only excluded genes that failed to reach an RPKM  
423 (reads per kilobase of exon model per million mapped reads) across all stages and organs higher  
424 than 1. Using WGCNA we built a signed network (based on the correlation across all stages and  
425 organs) using a power of 10 and default parameters. We then correlated the eigengenes for each  
426 module with the sample traits (i.e., organ and developmental stage).

427

428 We characterized each module in terms of biological processes and disease enrichments (GLAD4U)  
429 using the R implementation of WebGestalt (FDR ≤ 0.01; version 0.0.5) [37]. The lists of TFs are from

430 the animalTFDB (version 2.0) [17], the list of RNA-binding proteins are from the work of Gerstberger  
431 and colleagues [18], and the lists of genes from the main signaling pathways are from the following  
432 Gene Ontology (GO) categories: GO:0016055 (Wnt signaling pathway); GO:0007179 (transforming  
433 growth factor beta receptor signaling pathway); GO:0007224 (hedgehog signaling pathway);  
434 GO:0007169 (transmembrane receptor protein tyrosine kinase signaling pathway); GO:0030522  
435 (intracellular receptor signaling pathway); GO:0007259 (JAK-STAT cascade); and GO:0007219  
436 (Notch signaling pathway).

437

438 **Inherited disease genes**

439 The list of genes associated with human inherited disease was obtained from the manually curated  
440 HGMD (PRO 17.1) [23]. We only used genes with disease-causing mutations (DM tag; Table S2).  
441 Genes associated with DM mutations were mapped onto the Unified Medical Language System  
442 (UMLS), and aggregated into one or more of the following high level disease types: Eye, Nervous  
443 system, Reproductive, Cancer, Skin, Heart, Blood, Blood Coagulation, Endocrine, Immune, Digestive,  
444 Genitourinary, Metabolic, Ear Nose & Throat, Respiratory, Developmental, Musculoskeletal, and  
445 Psychiatric [23]. We also characterized the developmental profiles of 15 genes with dynamic  
446 temporal profiles in the brain that are associated with primary microcephaly (out of a set of 16 genes  
447 associated with this condition [38]), 171 associated with autism (out of 233 [39]) and 46 associated  
448 with schizophrenia (out of 75 [40]; we only considered loci where at most two genes were  
449 associated with the causative variant). There were only 7 genes with dynamic temporal profiles in  
450 the brain associated with both autism and schizophrenia. The list of human essential genes was  
451 obtained from the work of Bartha and colleagues [22].

452

453 The time- and organ-specificity indexes were based on the Tau metric of tissue-specificity [41] and  
454 were retrieved from the developmental resource [13]. Both indexes range from 0 (broad expression)  
455 to 1 (restricted expression). The pleiotropy index is to the number of samples where a gene is  
456 expressed ( $RPKM > 1$ ) over the total number of samples.

457

458 The most common temporal profiles in each organ were identified using the soft-clustering  
459 approach (c-means) implemented in the R package mFuzz (2.32.0) [42,43]. The clustering was  
460 restricted to genes previously identified as showing significant temporal differential expression in  
461 each organ (i.e., developmentally dynamic genes) [13]. We used as input the VS-transformed  
462 counts. The number of clusters was set to 6-8 depending on the organ.

463 **Comparing developmental trajectories**

464 For each organ, we compared the developmental trajectories of orthologous genes previously  
465 identified as showing significant temporal differential expression [13]. We used as input the VS-  
466 transformed counts (median across replicates) for matching stages between human and each of the  
467 other species. The developmental stage correspondences across species were retrieved from the  
468 developmental resource [13]. We used GPClust [44–46], which clusters time-series using Gaussian  
469 processes, to cluster the combined data for human and each of the other species. We set the noise  
470 variance (`k2.variance.fix`) to 0.7 and let GPClust infer the number of clusters. For each gene, GPClust  
471 assigned the probability of it belonging to each of the clusters. Therefore, for each gene we obtained  
472 a vector of probabilities that could be directly compared between pairs of 1:1 orthologs. We  
473 calculated the probability that pairs of orthologs were in the same cluster and used an FDR cut off  
474 of 5% to identify the genes that differed in trajectory between human and each of the other species.  
475 In Tables S3-S8, we provide for each organ and species the *P*-values (adjusted for multiple testing  
476 using the Benjamini-Hochberg procedure [47]) for the null hypothesis that orthologs have the same  
477 trajectory, and their classification as ‘same’ or ‘different’ based on an FDR of 5%.

478

479 General statistics and plots. Statistical analyses and plots were done in R (3.3.2) [48]. Plots were  
480 created using the R packages ggplot2 (2.2.1) [49], gridExtra (2.2.1) [50], reshape2 (1.4.2) [51], plyr  
481 (1.8.4) [52], and factoextra (1.0.4) [53].

482

483 **References**

- 484 1. Silbereis, J.C., Pochareddy, S., Zhu, Y., Li, M., and Sestan, N. (2016). The Cellular and  
485 Molecular Landscapes of the Developing Human Central Nervous System. *Neuron* **89**, 248.
- 486 2. Wang, V.Y., and Zoghbi, H.Y. (2001). Genetic regulation of cerebellar development. *Nat.*  
487 *Rev. Neurosci.* **2**, 484–491.
- 488 3. Bruneau, B.G. (2013). Signaling and Transcriptional Networks in Heart Development and  
489 Regeneration. *Cold Spring Harb Perspect Biol* **5**, a008292.
- 490 4. Si-tayeb, K., Lemaigre, P., and Duncan, S.A. (2016). Organogenesis and Development of the  
491 Liver. *Dev. Cell* **18**, 175–189.
- 492 5. DeFalco, T., and Capel, B. (2009). Gonad Morphogenesis in Vertebrates: Divergent Means to  
493 a Convergent End. *Annu. Rev. Cell Dev. Biol.* **25**, 457–482.
- 494 6. Vainio, S., and Lin, Y. (2002). Coordinating early kidney development: lessons from gene  
495 targeting. *Nat. Rev. Genet.* **3**, 533–543.

- 496 7. Pantalacci, S., and Semon, M. (2014). Transcriptomics of Developing Embryos and Organs: A  
497 Raising Tool for EvoDevo. *J. Exp. Zool.*, 1–9.
- 498 8. Lein, E.S., Belgard, T.G., Hawrylycz, M., and Molnár, Z. (2017). Transcriptomic Perspectives  
499 on Neocortical Structure, Development, Evolution, and Disease. *Annu. Rev. Neurosci.* **40**,  
500 629–652.
- 501 9. Bakken, T.E., Miller, J.A., Ding, S.L., Sunkin, S.M., Smith, K.A., Ng, L., Szafer, A., Dalley, R.A.,  
502 Royall, J.J., Lemon, T., *et al.* (2016). A comprehensive transcriptional map of primate brain  
503 development. *Nature* **535**, 367–375.
- 504 10. Zhu, Y., Sousa, A.M.M., Gao, T., Skarica, M., Li, M., Santpere, G., Esteller-Cucala, P., Juan, D.,  
505 Ferrández-Peral, L., Gulden, F.O., *et al.* (2018). Spatiotemporal transcriptomic divergence  
506 across human and macaque brain development. *Science* (80- ). 362.
- 507 11. Houmard, B., Small, C., Yang, L., Naluai-Cecchini, T., Cheng, E., Hassold, T., and Griswold, M.  
508 (2009). Global Gene Expression in the Human Fetal Testis and Ovary. *Biol. Reprod.* **81**, 438–  
509 443.
- 510 12. Giudice, J., Xia, Z., Wang, E.T., Scavuzzo, M.A., Ward, A.J., Kalsotra, A., Wang, W., Wehrens,  
511 X.H.T., Burge, C.B., Li, W., *et al.* (2014). Alternative splicing regulates vesicular trafficking  
512 genes in cardiomyocytes during postnatal heart development. *Nat. Commun.* **5**, 1–15.  
513 Available at: <http://dx.doi.org/10.1038/ncomms4603>.
- 514 13. Cardoso-Moreira, M., Halbert, J., Valloton, D., Velten, B., Chen, C., Shao, Y., Liechti, A.,  
515 Ascenção, K., Rummel, C., Ovchinnikova, S., *et al.* (2019). Gene expression across  
516 mammalian organ development. *Nature* **571**, 505–509.
- 517 14. Finucane, H.K., Reshef, Y.A., Anttila, V., Slowikowski, K., Gusev, A., Byrnes, A., Gazal, S., Loh,  
518 P.R., Lareau, C., Shores, N., *et al.* (2018). Heritability enrichment of specifically expressed  
519 genes identifies disease-relevant tissues and cell types. *Nat. Genet.* **50**, 621–629.
- 520 15. Li, M., Santpere, G., Kawasawa, Y.I., Evgrafov, O. V., Gulden, F.O., Pochareddy, S., Sunkin,  
521 S.M., Li, Z., Shin, Y., Zhu, Y., *et al.* (2018). Integrative functional genomic analysis of human  
522 brain development and neuropsychiatric risks. *Science* (80- ). 362, eaat7615.
- 523 16. Gerrelli, D., Liso, S., Copp, A.J., and Lindsay, S. (2015). Enabling research with human  
524 embryonic and fetal tissue resources. *Development* **142**, 3073–3076.
- 525 17. Zhang, H., Liu, T., Liu, C., Song, S., Zhang, X., Liu, W., Jia, H., Xue, Y., and Guo, A. (2014).  
526 AnimalTFDB 2 . 0 : a resource for expression , prediction and functional study of animal  
527 transcription factors. *Nucleic Acids Res.* **43**, D76–D81.
- 528 18. Gerstberger, S., Hafner, M., and Tuschl, T. (2014). A census of human RNA-binding proteins.

- 529            Nat. Rev. Genet. 15, 829–845.
- 530    19. Sarropoulos, I., Marin, R., Cardoso-moreira, M., and Kaessmann, H. (2019). Developmental  
531        dynamics of lncRNAs across mammalian organs and species. Nature 571, 510–514.
- 532    20. Stoeger, T., Gerlach, M., Morimoto, R.I., and Nunes Amaral, L.A. (2018). Large-scale  
533        investigation of the reasons why potentially important genes are ignored. PLoS Biol. 16, 1–  
534        25.
- 535    21. Mallo, M., Wellik, D.M., and Deschamps, J. (2010). Hox genes and regional patterning of the  
536        vertebrate body plan. Dev. Biol. 344, 7–15.
- 537    22. Bartha, I., Di Iulio, J., Venter, J.C., and Telenti, A. (2018). Human gene essentiality. Nat. Rev.  
538        Genet. 19, 51–62.
- 539    23. Stenson, P.D., Mort, M., Ball, E. V., Evans, K., Hayden, M., Heywood, S., Hussain, M., Phillips,  
540        A.D., and Cooper, D.N. (2017). The Human Gene Mutation Database: towards a  
541        comprehensive repository of inherited mutation data for medical research, genetic  
542        diagnosis and next-generation sequencing studies. Hum. Genet. 136, 665–677.
- 543    24. Lage, K., Hansen, N.T., Karlberg, E.O., Eklund, A.C., Roque, F.S., Donahoe, P.K., Szallasi, Z.,  
544        Jensen, T.S., and Brunak, S. (2008). A large-scale analysis of tissue-specific pathology and  
545        gene expression of human disease genes and complexes. Proc. Natl. Acad. Sci. 105, 20870–  
546        20875.
- 547    25. Barshir, R., Hekselman, I., Shemesh, N., Sharon, M., Novack, L., and Yeger-Lotem, E. (2018).  
548        Role of duplicate genes in determining the tissue-selectivity of hereditary diseases. PLoS  
549        Genet. 14, e1007327.
- 550    26. Omer Javed, A., Li, Y., Muffat, J., Su, K.C., Cohen, M.A., Lungjangwa, T., Aubourg, P.,  
551        Cheeseman, I.M., and Jaenisch, R. (2018). Microcephaly Modeling of Kinetochore Mutation  
552        Reveals a Brain-Specific Phenotype. Cell Rep. 25, 368–382.e5.
- 553    27. Stergachis, A.B., Neph, S., Sandstrom, R., Haugen, E., Reynolds, A.P., Zhang, M., Byron, R.,  
554        Canfield, T., Stelhing-Sun, S., Lee, K., et al. (2014). Conservation of trans-acting circuitry  
555        during mammalian regulatory evolution. Nature 515, 365–370.
- 556    28. Ta-Shma, A., El-lahham, N., Edvardson, S., Stepensky, P., Nir, A., Perles, Z., Gavri, S.,  
557        Golender, J., Yaakobi-Simhayoff, N., Shaag, A., et al. (2014). Conotruncal malformations and  
558        absent thymus due to a deleterious NKX2-6 mutation. J. Med. Genet. 51, 268–270.
- 559    29. Bello, S.M., Smith, C.L., and Eppig, J.T. (2015). Allele, phenotype and disease data at Mouse  
560        Genome Informatics: improving access and analysis. Mamm. Genome 26, 285–294.
- 561    30. Aridon, P., Marini, C., Di Resta, C., Brilli, E., De Fusco, M., Politi, F., Parrini, E., Manfredi, I.,

- 562 Pisano, T., Pruna, D., *et al.* (2006). Increased Sensitivity of the Neuronal Nicotinic Receptor  
563 α2 Subunit Causes Familial Epilepsy with Nocturnal Wandering and Ictal Fear. *Am. J. Hum.*  
564 *Genet.* **79**, 342–350.
- 565 31. Conti, V., Aracri, P., Chiti, L., Brusco, S., Mari, F., Marini, C., Albanese, M., Marchi, A., Liguori,  
566 C., Placidi, F., *et al.* (2015). Nocturnal frontal lobe epilepsy with paroxysmal arousals due to  
567 CHRNA2 loss of function. *Neurology* **84**, 1520–1528.
- 568 32. Kumar, S., Stecher, G., Suleski, M., and Hedges, S.B. (2017). TimeTree: A Resource for  
569 Timelines, Timetrees, and Divergence Times. *Mol. Biol. Evol.* **34**, 1812–1819.
- 570 33. Kosiol, C., Vinař, T., Da Fonseca, R.R., Hubisz, M.J., Bustamante, C.D., Nielsen, R., and Siepel,  
571 A. (2008). Patterns of positive selection in six mammalian genomes. *PLoS Genet.* **4**,  
572 e1000144.
- 573 34. Xue, Z., Huang, K., Cai, C., Cai, L., Jiang, C.Y., Feng, Y., Liu, Z., Zeng, Q., Cheng, L., Sun, Y.E., *et*  
574 *al.* (2013). Genetic programs in human and mouse early embryos revealed by single-cell  
575 RNA sequencing. *Nature* **500**, 593–597.
- 576 35. Langfelder, P., and Horvath, S. (2008). WGCNA: an R package for weighted correlation  
577 network analysis. *BMC Bioinformatics* **9**, 559.
- 578 36. Love, M.I., Anders, S., and Huber, W. (2014). Differential analysis of count data - the DESeq2  
579 package. *Genome Biol.* **15**, 10–1186.
- 580 37. Wang, J., Vasaikar, S., Shi, Z., Greer, M., and Zhang, B. (2017). WebGestalt 2017: A more  
581 comprehensive, powerful, flexible and interactive gene set enrichment analysis toolkit.  
582 *Nucleic Acids Res.* **45**, W130–W137.
- 583 38. Verloes, A., Drunat, S., Gressens, P., and Passemard, S. (1993). Primary autosomal recessive  
584 microcephalies and seckel syndrome spectrum disorders. In *GeneReviews*, M. P. Adam, ed.  
585 (University of Washington, Seattle).
- 586 39. Iossifov, I., Levy, D., Allen, J., Ye, K., Ronemus, M., Lee, Y., Yamrom, B., and Wigler, M.  
587 (2015). Low load for disruptive mutations in autism genes and their biased transmission.  
588 *Proc. Natl. Acad. Sci.* **112**, E5600–E5607.
- 589 40. Ripke, S., Neale, B.M., Corvin, A., Walters, J.T.R., Farh, K.H., Holmans, P.A., Lee, P., Bulik-  
590 Sullivan, B., Collier, D.A., Huang, H., *et al.* (2014). Biological insights from 108 schizophrenia-  
591 associated genetic loci. *Nature* **511**, 421–427.
- 592 41. Yanai, I., Benjamin, H., Shmoish, M., Chalifa-caspi, V., Shklar, M., Ophir, R., Bar-even, A.,  
593 Horn-saban, S., Safran, M., Domany, E., *et al.* (2005). Genome-wide midrange transcription  
594 profiles reveal expression level relationships in human tissue specification. *Bioinformatics*

- 595            21, 650–659.
- 596    42. Futschik, M.E., and Carlisle, B. (2005). Noise-Robust Soft Clustering of Gene Expression  
597            Time-Course Data. *J. Bioinform. Comput. Biol.* *03*, 965–988.
- 598    43. Kumar, L., and Futschik, M.E. (2012). Mfuzz: A software package for soft clustering of  
599            microarray data. *Bioinformation* *2*, 5–7.
- 600    44. Hensman, J., Rattray, M., and Lawrence, N.D. (2012). Fast Variational Inference in the  
601            Conjugate Exponential Family. In *Advances in neural information processing systems*, pp.  
602            2888–2896.
- 603    45. Hensman, J., Lawrence, N.D., and Rattray, M. (2013). Hierarchical Bayesian modelling of  
604            gene expression time series across irregularly sampled replicates and clusters. *BMC  
605            Bioinformatics* *14*, 252.
- 606    46. Hensman, J., Rattray, M., and Lawrence, N.D. (2015). Fast nonparametric clustering of  
607            structured time-series. *IEEE Trans. Pattern Anal. Mach. Intell.* *37*, 383–393.
- 608    47. Benjamini, Y., and Hochberg, Y. (1995). Controlling the False Discovery Rate: A Practical and  
609            Powerful Approach to Multiple Testing. *J. R. Stat. Soc. Ser. B* *57*, 289–300.
- 610    48. R Core Team (2014). R: A language and environment for statistical computing.
- 611    49. Wickham, H. (2009). *ggplot2: Elegant Graphics for Data Analysis* (New York: Springer-Verlag  
612            New York).
- 613    50. Auguie, B. (2016). *gridExtra: Miscellaneous Functions for “Grid” Graphics*. R package version  
614            2.2. 1.
- 615    51. Wickham, H. (2007). Reshaping Data with the reshape Package. *J. Stat. Softw.* *21*, 1–20.
- 616    52. Wickham, H. (2011). The split-apply-combine strategy for data analysis. *J. Stat. Softw.* *40*, 1–  
617            29.
- 618    53. Kassambara, A., and Mundt, F. (2017). *Factoextra: extract and visualize the results of  
619            multivariate data analyses*.
- 620

621 **Supplementary figure legends**

622 **Figure S1. Human weighted gene co-expression network. (A)** Organ developmental profiles for  
623 each module; shown is the module’s eigengene. **(B)** Modules with a high fraction of TFs are  
624 associated with expression in early development whereas modules with a low fraction of TFs are  
625 associated with expression in late development. Shaded area corresponds to the 95% confidence  
626 interval. **(C)** There is a strong positive correlation between the fraction of developmentally dynamic  
627 lncRNAs in a module and the fraction of poorly studied protein-coding genes. Poorly studied genes

628 are those with 3 or fewer publications (left) or those with 8 or fewer publications (right). Data on  
629 the number of publications are from Stoeger and colleagues. Shaded area corresponds to the 95%  
630 confidence interval.

631

632 **Figure S2. Breadth of developmental expression of key groups of developmental genes.** Time and  
633 organ-specificity of selected sets of TFs, signaling genes and RBPs. Both indexes range from 0 (broad  
634 expression) to 1 (restricted expression) (Methods). The boxplots depict the median ± 25th and 75th  
635 percentiles, whiskers at 1.5 times the interquartile range.

636

637 **Figure S3. Spatiotemporal profile of time and/or organ-specific RBPs** (organ- and/or median time-  
638 specificity  $\geq 0.8$ ). In each organ, the samples are ordered from early to late development.

639

640 **Figure S4. Spatiotemporal profiles of TFs with a Myb DNA binding domain.** In each organ, the  
641 samples are ordered from early to late development.

642

643 **Figure S5. Spatiotemporal profiles of TFs with a POU domain.** In each organ, the samples are  
644 ordered from early to late development.

645

646 **Figure S6. Spatiotemporal profiles of TFs with a Forkhead domain.** In each organ, the samples are  
647 ordered from early to late development.

648

649 **Figure S7. Spatiotemporal profiles of Hox genes.** In each organ, the samples are ordered from early  
650 to late development.

651

652 **Figure S8. Spatiotemporal profiles of disease genes.** **(A)** Organ- and time-specificity (median across  
653 organs) for genes in different classes of phenotypic severity (P-values from Wilcoxon rank sum test,  
654 two-sided). The boxplots depict the median ± 25th and 75th percentiles, whiskers at 1.5 times the  
655 interquartile range. **(B)** Distribution of genes associated with heart disease among the 6 heart  
656 clusters. Cluster 1 is enriched for heart disease-associated genes both when using all genes  
657 associated with a heart phenotype ( $n = 230$ ) and when restricting the set to those exclusively  
658 associated with the heart ( $n = 46$ ) (P-values from binomial tests). **(C)** Distribution of genes associated  
659 with metabolic diseases among the 6 liver clusters. Cluster 5 is enriched for metabolic disease-  
660 associated genes both when using all genes associated with a metabolic phenotype ( $n = 379$ ) and

661 when restricting the set to those exclusively associated with metabolism ( $n = 103$ ) ( $P$ -values from  
662 binomial tests).

663

664 **Figure S9. Spatiotemporal profiles of disease genes.** **(A)** Number of organs where genes have  
665 dynamic temporal profiles as a function of the number of organs where they are known to cause  
666 disease. **(B)** Time-specificity in different organs for genes associated exclusively with  
667 neurodevelopmental phenotypes. **(C)** Relationship between human and mouse expression  
668 pleiotropy. The blue dots denote disease-associated genes and the orange dots denote disease-  
669 associated genes expressed in at least 50% of the samples in one species but in less than 10% of the  
670 samples in the other. In **(A)** and **(B)** the boxplots depict the median  $\pm$  25th and 75th percentiles,  
671 whiskers at 1.5 times the interquartile range.

672

### 673 **Supplementary table legends**

674 **Table S1.** Top 5 biological processes and disease enrichments (FDR < 1%, hypergeometric test) for  
675 each of the 32 modules in the gene co-expression network.

676

677 **Table S2.** Lists of human genes, the modules to which they belong in the global gene co-expression  
678 network, the clusters to which they were assigned in each organ (soft clustering), their associations  
679 with disease ('DM' means disease-causing), the number of organs where they show dynamic  
680 temporal profiles, the organ of maximal expression during development, their organ- and time-  
681 specificity, and their global expression pleiotropy.

682

683 **Table S3.** Comparison of brain temporal trajectories between human genes and their orthologs in  
684 mouse, rat, rabbit, and rhesus macaque. Trajectories were called different when the adjusted  
685 probability of the orthologs being in the same cluster is  $\leq 0.05$ . Only genes with dynamic temporal  
686 profiles in the brain of humans and at least one of the other species were tested for trajectory  
687 differences.

688

689 **Table S4.** Comparison of cerebellum temporal trajectories between human genes and their  
690 orthologs in mouse, rat, and rabbit. Trajectories were called different when the adjusted probability  
691 of the orthologs being in the same cluster is  $\leq 0.05$ . Only genes with dynamic temporal profiles in  
692 the cerebellum of humans and at least one of the other species were tested for trajectory  
693 differences.

694

695 **Table S5.** Comparison of heart temporal trajectories between human genes and their orthologs in  
696 mouse, rat, rabbit, and rhesus macaque. Trajectories were called different when the adjusted  
697 probability of the orthologs being in the same cluster is  $\leq 0.05$ . Only genes with dynamic temporal  
698 profiles in the heart of humans and at least one of the other species were tested for trajectory  
699 differences.

700

701 **Table S6.** Comparison of kidney temporal trajectories between human genes and their orthologs in  
702 mouse, rat, and rabbit. Trajectories were called different when the adjusted probability of the  
703 orthologs being in the same cluster is  $\leq 0.05$ . Only genes with dynamic temporal profiles in the  
704 kidney of humans and at least one of the other species were tested for trajectory differences.

705

706 **Table S7.** Comparison of liver temporal trajectories between human genes and their orthologs in  
707 mouse, rat, rabbit, and rhesus macaque. Trajectories were called different when the adjusted  
708 probability of the orthologs being in the same cluster is  $\leq 0.05$ . Only genes with dynamic temporal  
709 profiles in the liver of humans and at least one of the other species were tested for trajectory  
710 differences.

711

712 **Table S8.** Comparison of testis temporal trajectories between human genes and their orthologs in  
713 mouse, rat, and rabbit. Trajectories were called different when the adjusted probability of the  
714 orthologs being in the same cluster is  $\leq 0.05$ . Only genes with dynamic temporal profiles in the testis  
715 of humans and at least one of the other species were tested for trajectory differences.

716

717 **Table S9.** Organs, developmental stages, and number of replicates sampled in each species.

718

# Figure S1

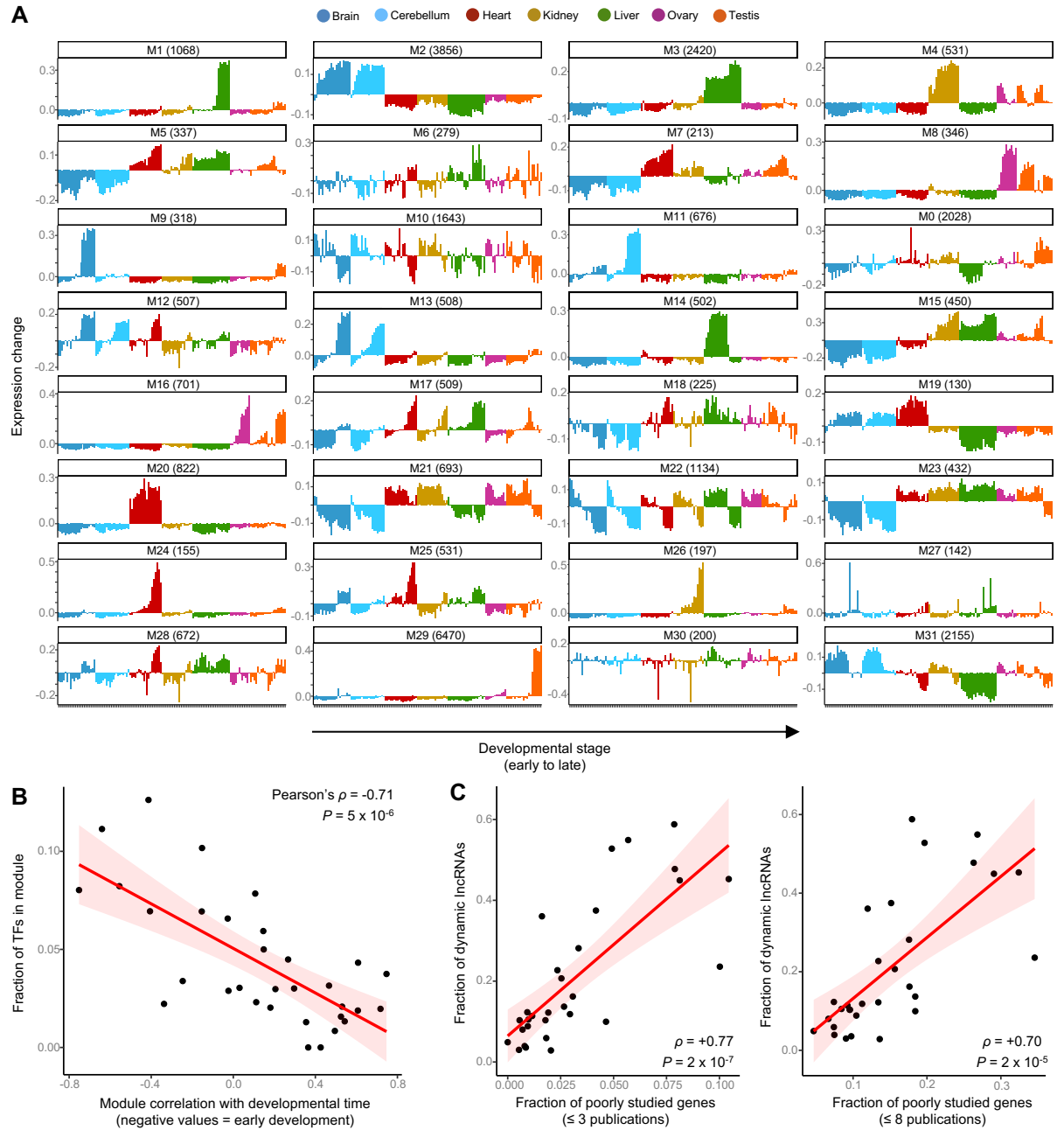


**Figure S1: Human weighted gene co-expression network.** (A) Organ developmental profiles for each module; shown is the module's eigengene. (B) Modules with a high fraction of TFs are associated with expression in early development whereas modules with a low fraction of TFs are associated with expression in late development. Shaded area corresponds to the 95% confidence interval. (C) There is a strong positive correlation between the fraction of developmentally dynamic lncRNAs in a module and the fraction of poorly studied protein-coding genes. Poorly studied genes are those with 3 or fewer publications (left) or those with 8 or fewer publications (right). Data on the number of publications are from Stoeger and colleagues<sup>16</sup>. Shaded area corresponds to the 95% confidence interval.

# Figure S2

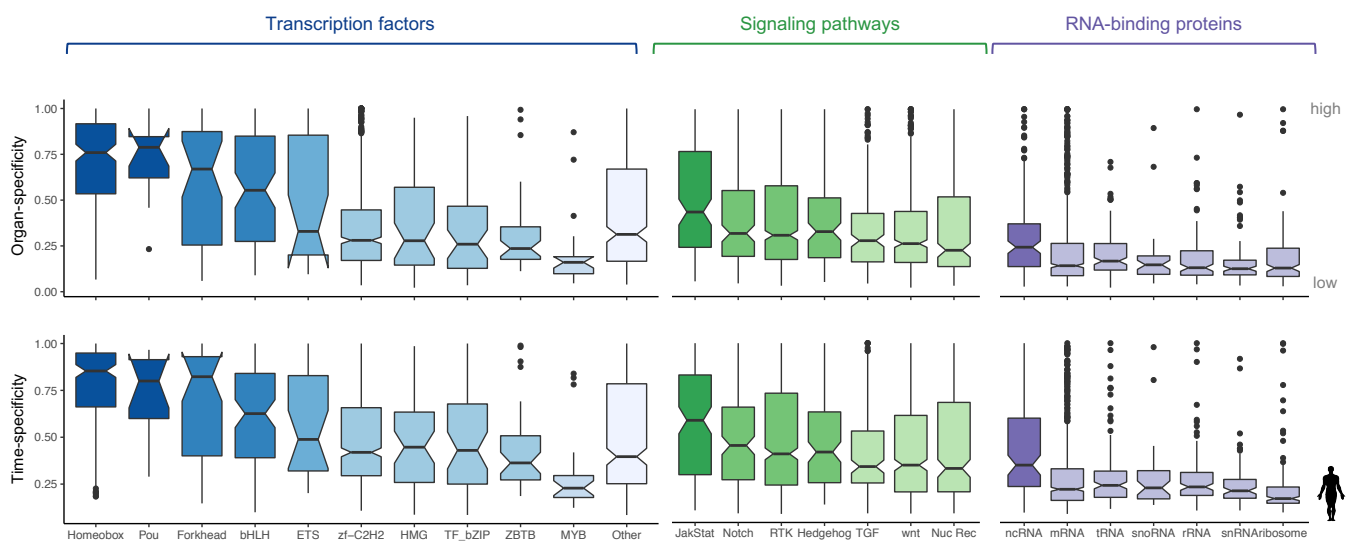


**Figure S2. Breadth of developmental expression of key groups of developmental genes.** Time and organ-specificity of selected sets of TFs, signaling genes and RBPs. Both indexes range from 0 (broad expression) to 1 (restricted expression) (Methods). The box plots depict the median  $\pm$  25th and 75th percentiles, whiskers at 1.5 times the interquartile range.

Figure S3

### RBPs: time and/or tissue-specific

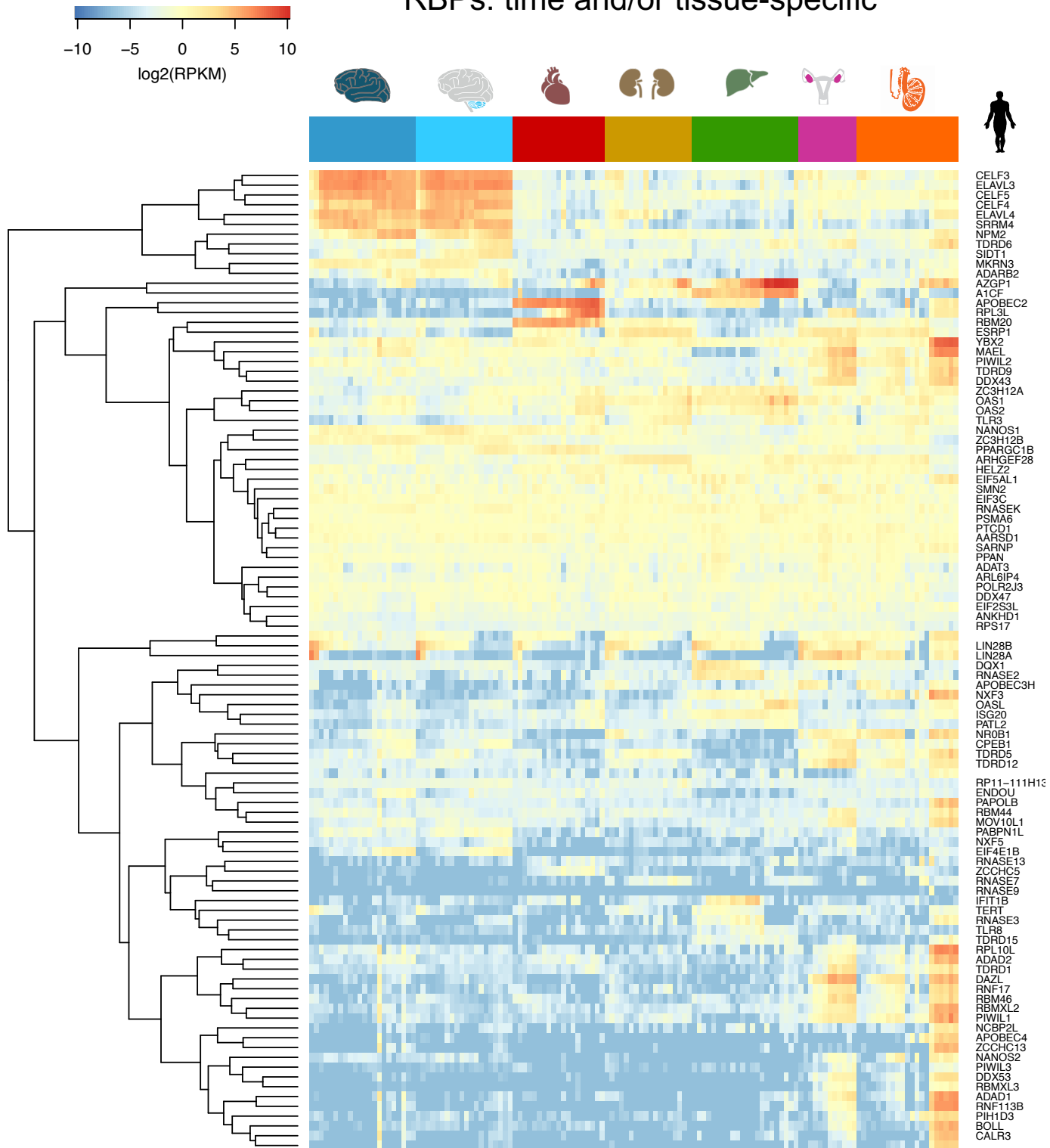


**Figure S3. Spatiotemporal profiles of time and/or organ-specific RBPs (organ- and/or median time-specificity  $\geq 0.8$ ).** In each organ, the samples are ordered from early to late development.

**Figure S4**

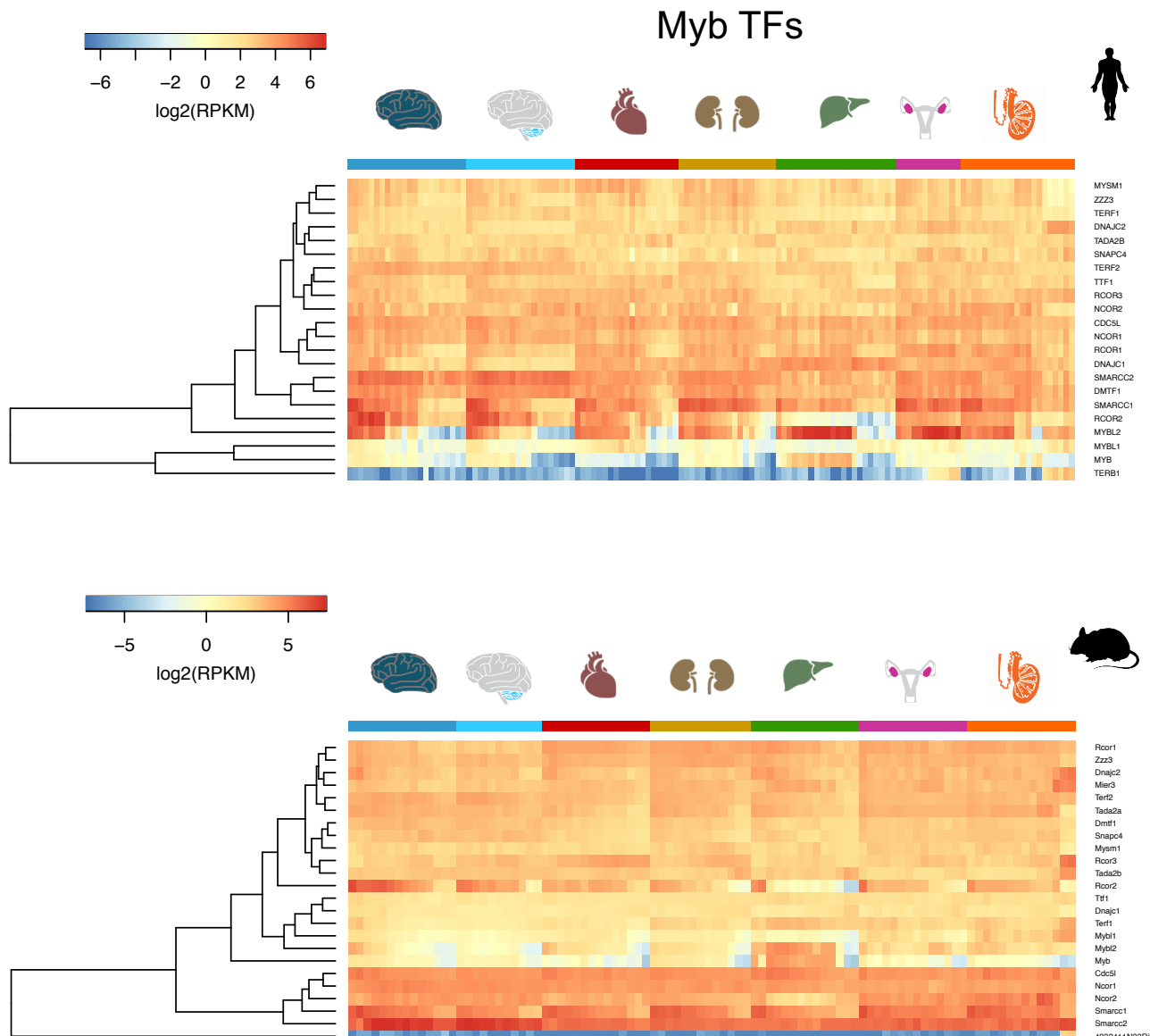


**Figure S4. Spatiotemporal profiles of TFs with a Myb DNA binding domain.** In each organ, the samples are ordered from early to late development.

Figure S5

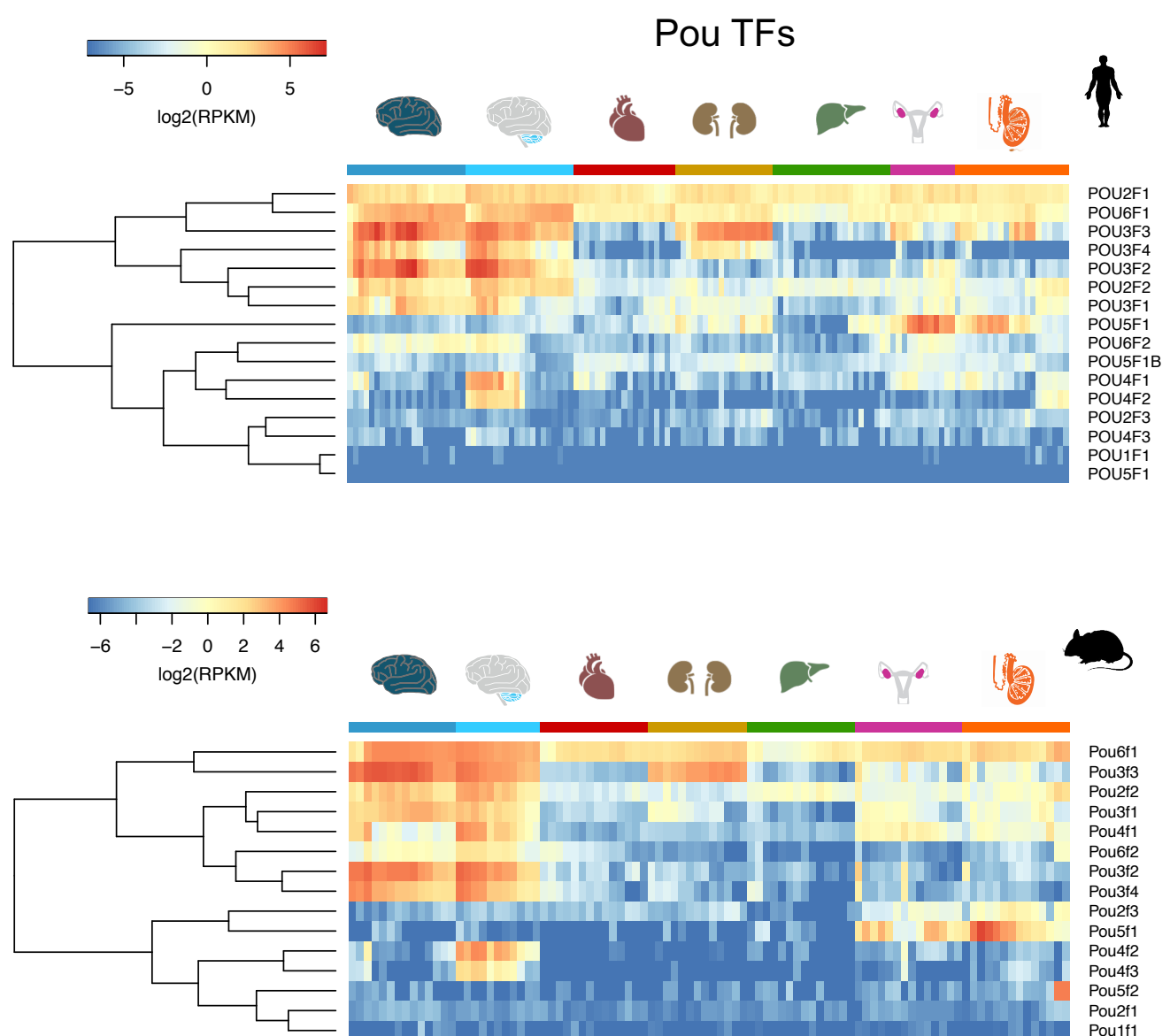
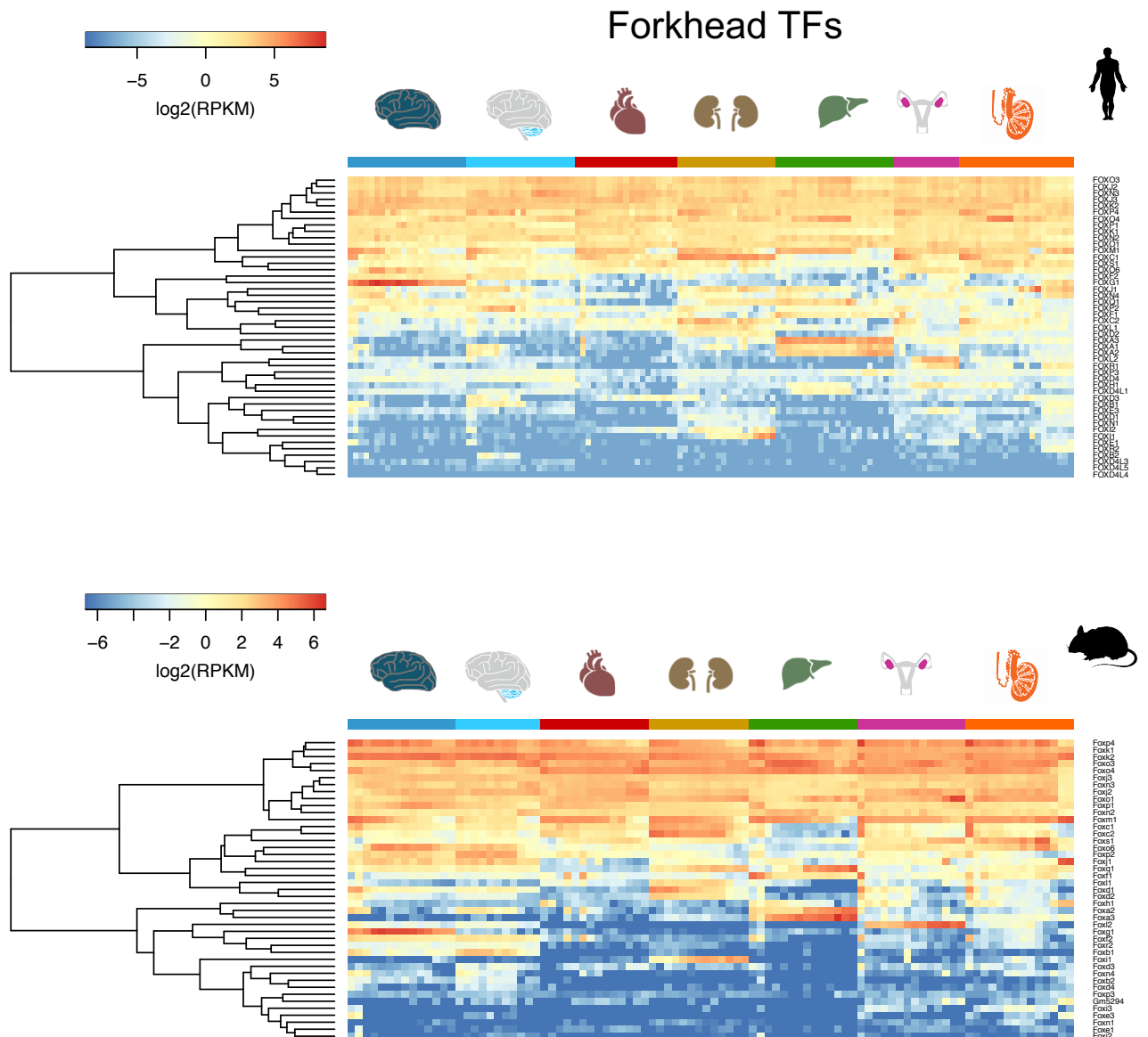


Figure S5. Spatiotemporal profiles of TFs with a POU domain. In each organ, the samples are ordered from early to late development.

**Figure S6**



**Figure S6: Spatiotemporal profiles of TFs with a Forkhead domain.** In each organ, the samples are ordered from early to late development.

Figure S7

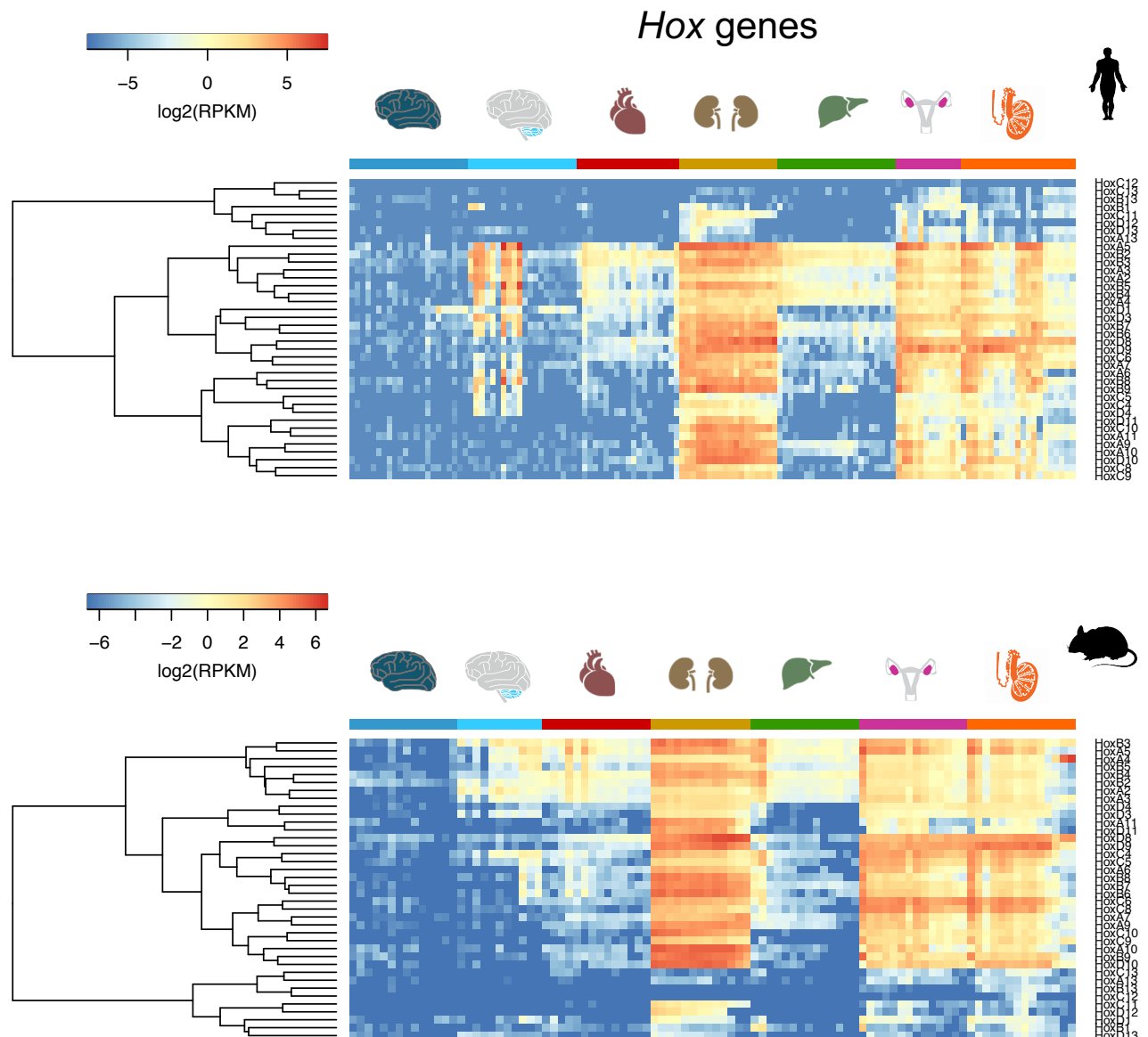
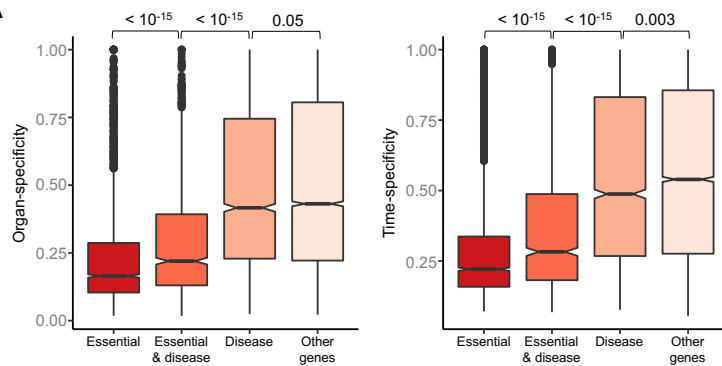


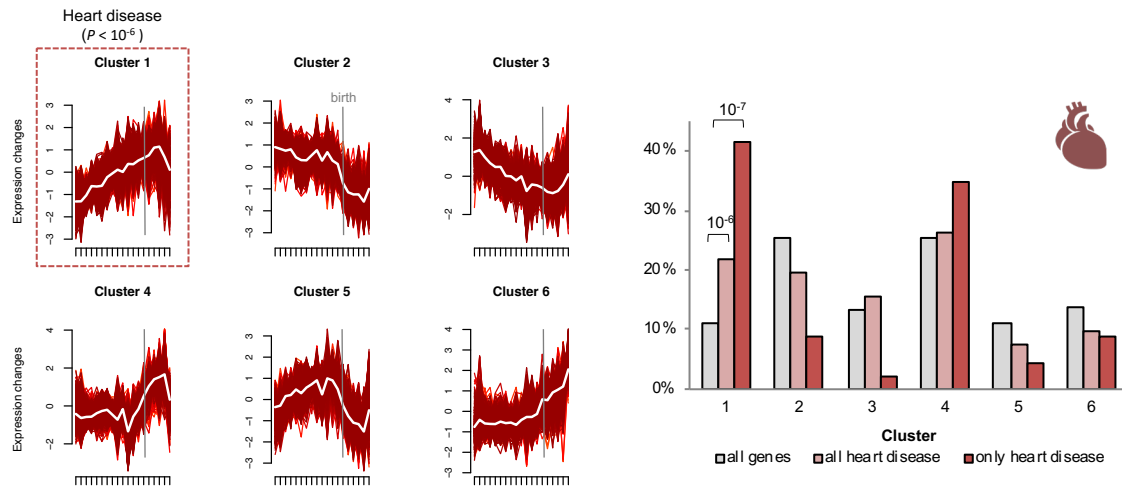
**Figure: Spatiotemporal profiles of *Hox* genes.** In each organ, the samples are ordered from early to late development.

# Figure S8

**A**



**B**



**C**

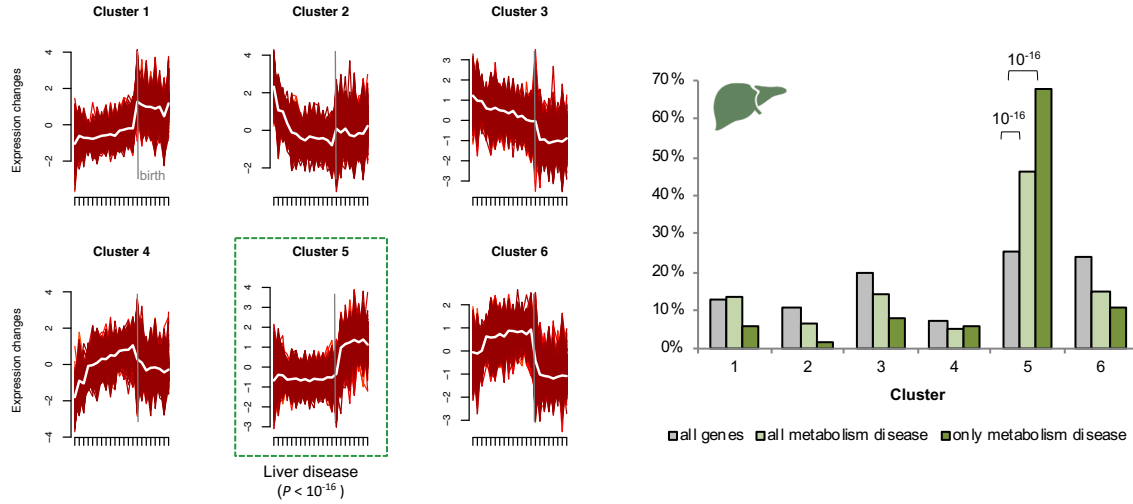


**Figure S8. Spatiotemporal profiles of disease genes.** **(A)** Organ- and time-specificity (median across organs) for genes in different classes of phenotypic severity (P-values from Wilcoxon rank sum test, two-sided). The box plots depict the median  $\pm$  25th and 75th percentiles, whiskers at 1.5 times the interquartile range. **(B)** Distribution of genes associated with heart disease among the 6 heart clusters. Cluster 1 is enriched for heart disease-associated genes both when using all genes associated with a heart phenotype ( $n = 230$ ) and when restricting the set to those exclusively associated with the heart ( $n = 46$ ) (P-values from binomial tests). **(C)** Distribution of genes associated with metabolic diseases among the 6 liver clusters. Cluster 5 is enriched for metabolic disease-associated genes both when using all genes associated with a metabolic phenotype ( $n = 379$ ) and when restricting the set to those exclusively associated with metabolism ( $n = 103$ ) (P-values from binomial tests).

# Figure S9

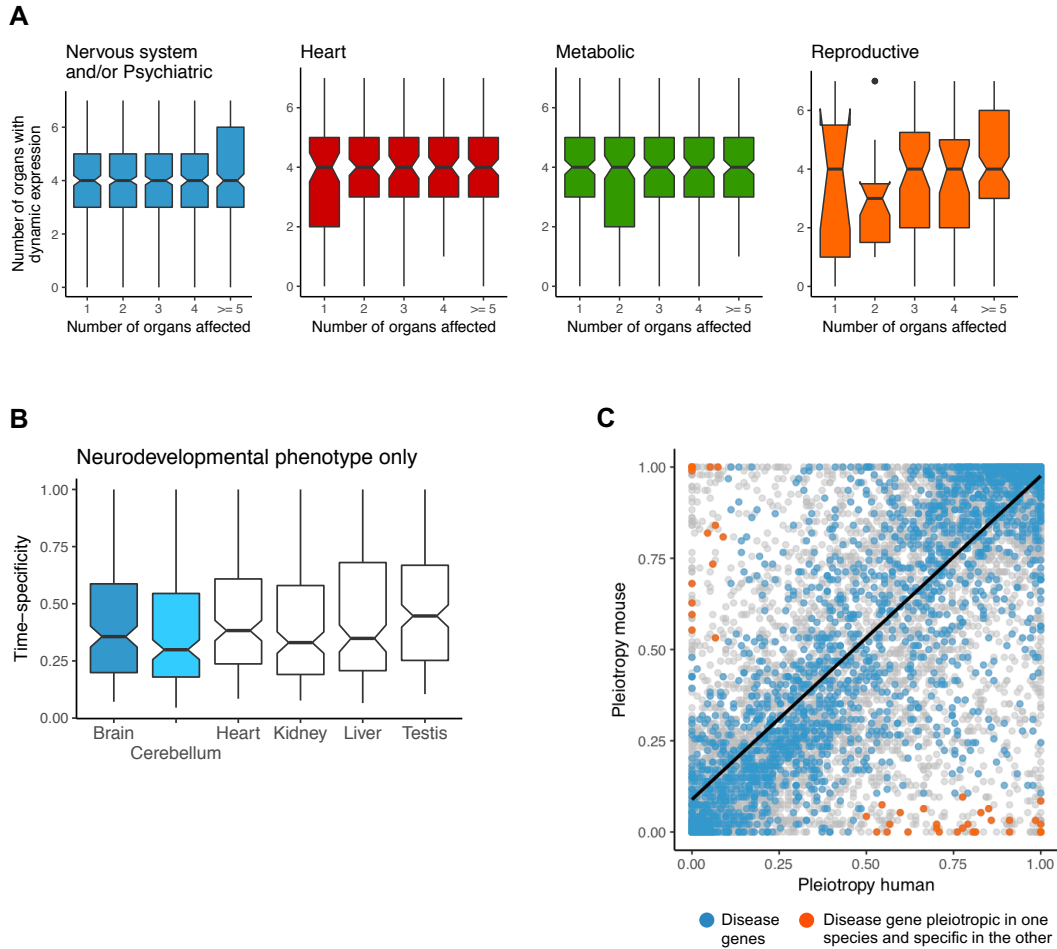


**Figure S9: Spatiotemporal profiles of disease genes.** (A) Number of organs where genes have dynamic temporal profiles as a function of the number of organs where they are known to cause disease. (B) Time-specificity in different organs for genes associated exclusively with neurodevelopmental phenotypes. (C) Relationship between human and mouse expression pleiotropy. The blue dots denote disease-associated genes and the orange dots denote disease-associated genes expressed in at least 50% of the samples in one species but in less than 10% of the samples in the other. In (A) and (B) the box plots depict the median  $\pm$  25th and 75th percentiles, whiskers at 1.5 times the interquartile range.